J Nonlinear Sci (2011) 21:875–895
DOI 10.1007/s00332-011-9103-4

Journal of Nonlinear Science

On Bifurcations in Nonlinear Consensus Networks

Vaibhav Srivastava · Jeff Moehlis · Francesco Bullo

Received: 28 April 2010 / Accepted: 9 June 2011 / Published online: 15 July 2011
© Springer Science+Business Media, LLC 2011

Abstract The theory of consensus dynamics is widely employed to study various linear behaviors in networked control systems. Moreover, nonlinear phenomena have been observed in animal groups, power networks and in other networked systems. These observations inspire the development in this paper of three novel approaches to define distributed nonlinear dynamical interactions. The resulting dynamical systems are akin to higher-order nonlinear consensus systems. Over connected undirected graphs, the resulting dynamical systems exhibit various interesting behaviors that we rigorously characterize.

Keywords Consensus network · Networked systems · Bifurcation theory

Mathematics Subject Classification (2000) 34C23 · 34K18 · 68M12

Communicated by R. Sepulchre.

A preliminary version of this work (Srivastava et al. 2010) was presented at the 2010 American Control Conference, Baltimore, MD, USA.

V. Srivastava (✉) · J. Moehlis · F. Bullo
Department of Mechanical Engineering, University of California Santa Barbara, Santa Barbara, CA 93106, USA
e-mail: vaibhav@engineering.ucsb.edu

J. Moehlis
e-mail: moehlis@engineering.ucsb.edu

F. Bullo
e-mail: bullo@engineering.ucsb.edu

1 Introduction

Collective behavior in animal groups, such as schools of fish, flocks of birds, and herds of wildebeests, is a widely studied phenomenon. It has been proposed that the decision making in such groups is distributed rather than central: each individual in such a group decides how to behave based on local information. In particular, some adjacency-based averaging models have been proposed to model the observed behavior in such systems. These adjacency-based averaging algorithms are called consensus algorithms, and they have been widely studied in various engineering applications.

Of particular interest are recent results in ecology (Couzin et al. 2005) which show that, for a small difference in the preferences of the individuals, the decision making in animal groups is well modeled using consensus dynamics. For significant differences in the preferences of individuals, the decision dynamics bifurcate away from consensus. This observation provides motivation for the development of dynamical systems which mimic such nonlinear behaviors in engineered multi-agent systems.

Recently, dynamical systems theory and control theory have been extensively applied to networked systems. In particular, the consensus problem has been studied in various fields, e.g., network synchronization (Papachristodoulou and Jadbabaie 2006), flocking (Tanner et al. 2007), rendezvous (Lin et al. 2007), sensor fusion (Spanos et al. 2005), formation control (Fax and Murray 2004), etc.; a detailed description is presented in Olfati-Saber et al. (2007), Jadbabaie et al. (2003). Some nonlinear phenomena have been studied in certain network classes. Certain nonlinear protocols to achieve consensus have been studied (Arcak 2007). The bifurcation problem has been studied in neural networks; a Hopf-like bifurcation has been observed in a two cell autonomous system (Zou and Nossek 1993), and pitchfork and Hopf bifurcations have been studied in artificial neural networks (Olien and Bélair 1997; Wei and Ruan 1999). Some static bifurcations have been studied in load flow dynamics of power networks (Kwatny et al. 1986). Hopf bifurcations in a network of interconnected systems have been studied (Dionne et al. 1996). Certain Kuramoto oscillator-based models have been proposed to model decision dynamics in animal groups, and the underlying bifurcations have been studied (Nabet et al. 2009). A version of bifurcations in consensus networks has been studied in the opinion dynamics literature (Lorenz 2007). The models in opinion dynamics problems can be interpreted as consensus dynamics on a time-varying graph with no globally reachable node. These models are complicated and difficult to implement on an engineered multi-agent network.

The human decision making models proposed in Bogacz et al. (2006) have been recently utilized in Poulakakis et al. (2010) to develop a Laplacian flow-based model of collective decision making in human groups. Related nonlinear models for human decision making have been developed in Roxin and Ledberg (2008). The dynamics in these models resemble those associated with a pitchfork bifurcation. In view of these examples of dynamics, we envision the need for frameworks to model the nonlinear interactions of multiple-agents.

Moreover, in formation control of a multi-agent system, the control laws are defined based on particular interactions among the agents (Dörfler and Francis 2010).

The interactions among the agents are based on the gradients of the potential functions. A generalized framework to study such interactions and design the potential functions that accomplish the desired final configuration still needs to be developed.

In this paper, we propose distributed algorithms to achieve nonlinear behaviors in a networked system. We define three frameworks, namely, the absolute nonlinear flow, the relative nonlinear flow, and the disagreement nonlinear flow, to define nonlinear dynamics on a multi-agent network. We apply these frameworks to the characterization of a pitchfork bifurcation in a multi-agent network. For a graph with a single node, the proposed dynamics reduce to scalar nonlinear dynamics. In essence, the proposed dynamics entail extensions of the scalar nonlinear dynamics to engineered multi-agent systems. The major contributions of our work are:

(1) We propose generalized frameworks to describe distributed nonlinear dynamics in a multi-agent network.
(2) For each framework, we generically define the set of final possible equilibrium configurations.
(3) We define the distributed pitchfork bifurcation dynamics for networked systems using these frameworks.
(4) We present some general tools to study the stability of these equilibria, and we utilize them to study the associated dynamics.
(5) We present a comprehensive treatment of these dynamics for low order networks.

The remainder of the paper is organized as follows. In Sect. 2, we elucidate some basics of dynamical systems and graph theory, which is followed by the development of frameworks to define nonlinear dynamics on graphs in Sect. 3. We use these frameworks to study pitchfork bifurcation dynamics on graphs in Sect. 4. Finally, our conclusions are presented in Sect. 5.

2 Preliminaries

2.1 Pitchfork Bifurcation

The equation

$$\dot{x} = \gamma x - x^3, \quad \gamma, x \in \mathbb{R}, \tag{1}$$

is defined as the normal form for the supercritical pitchfork bifurcation (Strogatz 2000). The dynamics of (1) are as follows:

(1) For $\gamma < 0$, there exists a stable equilibrium point at $x = 0$, and there is no other equilibrium point.
(2) For $\gamma = 0$, there exists a critically stable equilibrium point at $x = 0$.
(3) For $\gamma > 0$, there exist two stable equilibrium points at $x = \pm\sqrt{\gamma}$, and there is an unstable equilibrium point at $x = 0$.

The point $\gamma = 0$ is called the bifurcation point.

2.2 Laplacian Matrix of a Graph

Given a digraph $\mathcal{G} = (V, \mathcal{E})$, where $V = \{v_1, \ldots, v_n\}$ is the set of nodes and $\mathcal{E}$ is the set of edges, the *Laplacian matrix* $\mathcal{L}(\mathcal{G}) \in \mathbb{R}^{n\times n}$ has entries

$$l_{i,j} = \begin{cases} -1, & \text{if } (i, j) \in \mathcal{E}, \\ d_i, & \text{if } i = j, \\ 0, & \text{otherwise}, \end{cases}$$

where d_i is the out-degree of node i, i.e., number of edges emanating from node i (Bullo et al. 2009). The set of nodes $j \in V$, such that $(i, j) \in \mathcal{E}$, is referred to as the *adjacency* of the node i, and is denoted $\mathrm{adj}(i)$.

Properties of the Laplacian Matrix:

(1) The Laplacian matrix is symmetric if and only if $\mathcal{G}$ is undirected.
(2) A symmetric Laplacian matrix is positive semidefinite.
(3) For a graph $\mathcal{G}$ with n nodes and at least one globally reachable node, the rank of the Laplacian matrix is $n - 1$.
(4) The kernel of the Laplacian matrix for a graph $\mathcal{G}$ of order n with at least one globally reachable node is $\mathrm{diag}(\mathbb{R}^n)$, i.e. $\{(x_1, \ldots, x_n) \in \mathbb{R}^n \mid x_1 = \cdots = x_n\}$.

2.3 Center-Manifold Theorem

For $(z_1, z_2) \in \mathbb{R}^{n_1} \times \mathbb{R}^{n_2}$, consider the following system:

$$\begin{aligned} \dot{z}_1 &= A_1 z_1 + g_1(z_1, z_2), \\ \dot{z}_2 &= A_2 z_2 + g_2(z_1, z_2), \end{aligned} \tag{2}$$

where all eigenvalues of $A_1 \in \mathbb{R}^{n_1\times n_1}$ and $A_2 \in \mathbb{R}^{n_2\times n_2}$ have zero and negative real parts, respectively. The functions $g_1 : \mathbb{R}^{n_1} \times \mathbb{R}^{n_2} \to \mathbb{R}^{n_1}$, and $g_2 : \mathbb{R}^{n_1} \times \mathbb{R}^{n_2} \to \mathbb{R}^{n_2}$ satisfy the conditions

$$g_i(0, 0) = 0, \qquad \frac{\partial g_i}{\partial z}(0, 0) = 0, \quad \forall i \in \{1, 2\}. \tag{3}$$

For the system in (2), for small z_1, there exists (Khalil 2002) an invariant center manifold $h : \mathbb{R}^{n_1} \to \mathbb{R}^{n_2}$ satisfying the conditions

$$h(0) = 0, \qquad \frac{\partial h}{\partial z_1}(0) = 0, \quad \text{and}$$
$$A_2 h(z_1) + g_2\big(z_1, h(z_1)\big) = \frac{\partial h}{\partial z_1}(z_1)\big[A_1 z_1 + g_1\big(z_1, h(z_1)\big)\big].$$

The center-manifold theorem (Khalil 2002) states that the dynamics on the center manifold determine the overall asymptotic dynamics of (2) near $(z_1, z_2) = (0, 0)$, i.e., the overall dynamics are determined by

$$\dot{z}_1 = A_1 z_1 + g_1\big(z_1, h(z_1)\big). \tag{4}$$

2.4 Laplacian Flow

Let $\mathcal{G}$ be a undirected connected graph of order n. The *Laplacian flow* on $\mathbb{R}^n$ is defined by

$$\dot{x} = -\mathcal{L}(\mathcal{G})x.$$

In components, the Laplacian flow is given by

$$\dot{x}_i = \sum_{j \in \mathrm{adj}(i)} (x_j - x_i), \quad i \in \{1, \ldots, n\}.$$

The vector $\mathcal{L}(\mathcal{G})x$ is called the *disagreement vector*. It has been shown in Olfati-Saber and Murray (2004) that the solutions to the Laplacian flow converge to $\mathrm{diag}(\mathbb{R}^n)$, that is, to consensus, for fixed as well as switching topologies.

3 Distributed Nonlinear Dynamics in Networks

Before we define distributed nonlinear dynamics in networks, we introduce the following notation. We denote the set of connected undirected graphs with n nodes by

$$\Gamma_n = \big\{\mathcal{G} \mid \mathcal{L}(\mathcal{G}) = \mathcal{L}(\mathcal{G})^T, \text{ and } \mathrm{rank}\big(\mathcal{L}(\mathcal{G})\big) = n - 1\big\}.$$

3.1 Absolute Nonlinear Flow

We call a flow *absolute nonlinear flow* if each node transmits a value which is a function of only its own label. For a $\mathcal{G} \in \Gamma_n$, on $\mathbb{R}^n$, such a flow is given by

$$\dot{x} = \mathcal{L}(\mathcal{G}) f(x),$$

where $f : \mathbb{R}^n \to \mathbb{R}^n$ is a smooth function. In components, the absolute nonlinear flow is given by

$$\dot{x}_i = \sum_{j \in \mathrm{adj}(i)} \big(f_i(x_i) - f_j(x_j)\big), \quad \forall i \in \{1, \ldots, n\}.$$

The set of equilibrium points of the absolute nonlinear flow is

$$\big\{x^* \mid f(x^*) \in \mathrm{diag}\big(\mathbb{R}^n\big)\big\}.$$

The salient feature of the absolute nonlinear flow formulation is that the set of equilibrium points is an invariant over the set Γ_n. Moreover, the sum of the states is an invariant over any trajectory of the system, which follows from the fact that $\sum_{i=1}^n \dot{x}_i = 0$.

3.2 Relative Nonlinear Flow

We call a flow *relative nonlinear flow* if each node transmits a value which is determined only by the difference between the state of the node and the neighboring node. For a $\mathcal{G} \in \Gamma_n$, on $\mathbb{R}^n$, such a flow is given by

$$\dot{x}_i = \sum_{j \in \mathrm{adj}(i)} f_i(x_i - x_j), \quad \forall i \in \{1, \ldots, n\},$$

where $f_i : \mathbb{R} \to \mathbb{R},\ i \in \{1, \ldots, n\}$ are smooth functions.

3.3 Disagreement Nonlinear Flow

We call a flow a *disagreement nonlinear flow* if each node transmits a value which is determined only by the corresponding entry in the disagreement vector. For a $\mathcal{G} \in \Gamma_n$, on $\mathbb{R}^n$, such a flow is given by

$$\dot{x} = f\big(\mathcal{L}(\mathcal{G})x\big),$$

where $f : \mathbb{R}^n \to \mathbb{R}^n$ is some smooth function. In components, the disagreement nonlinear flow is given by

$$\dot{x}_i = f_i\Bigg(\sum_{j \in \mathrm{adj}(i)} (x_i - x_j)\Bigg), \quad \forall i \in \{1, \ldots, n\}.$$

A particular case of the disagreement nonlinear flow is when each f_i is a polynomial. In this scenario, the disagreement nonlinear flow is given by

$$\dot{x} = \big(a_0 + a_1 \mathcal{D}(x) + \cdots + a_m \big(\mathcal{D}(x)\big)^m\big)\mathbf{1}_n,$$

where $\mathcal{D}(x) = \mathrm{diag}\,(\mathcal{L}(\mathcal{G})x)$. In components, this becomes

$$\dot{x}_i = a_0 + a_1 \mathcal{I}(x_i) + \cdots + a_m \big(\mathcal{I}(x_i)\big)^m, \quad \forall i \in \{1, \ldots, n\},$$

where $\mathcal{I}(x_i) = \sum_{j \in \mathrm{adj}(i)} (x_i - x_j)$. Let the $r \leq m$ real roots of the equation

$$a_0 + a_1 z + \cdots + a_m z^m = 0$$

be z_i, $i \in \{1, \ldots, r\}$. The set of equilibrium points of the disagreement nonlinear flow with polynomial nonlinearity is

$$\big\{x^* \in \mathbb{R}^n \mid \big(\mathcal{L}(\mathcal{G})x^*\big)_i \in \{z_1, \ldots, z_r\}, \forall i \in \{1, \ldots, n\}\big\},$$

where $(\mathcal{L}(\mathcal{G})x^*)_i$ represents the ith entry of the vector $\mathcal{L}(\mathcal{G})x^*$. Here, the equilibrium points depend on the graph topology.

4 Distributed Bifurcation Dynamics in Networks

We study a particular class of distributed nonlinear dynamics where $f_i : \mathbb{R} \to \mathbb{R}$, for each $i \in \{1, \ldots, n\}$, is $f_i(x) = \gamma x - x^3$, where $\gamma \in \mathbb{R}$ is some constant. We refer to such a nonlinearity as a *pitchfork nonlinearity*.

4.1 Absolute Nonlinear Flow with Pitchfork Nonlinearity

Given a connected undirected graph $\mathcal{G} \in \Gamma_n$, and $\gamma \in \mathbb{R}$, the absolute nonlinear flow with pitchfork nonlinearity is

$$\dot{x} = \gamma \mathcal{L}(\mathcal{G})x - \mathcal{L}(\mathcal{G}) \operatorname{diag}(x)^3 \mathbf{1}_n. \tag{5}$$

In components, this becomes

$$\dot{x}_i = \gamma \sum_{j \in \operatorname{adj}(i)} (x_i - x_j) - \sum_{j \in \operatorname{adj}(i)} \left(x_i^3 - x_j^3\right), \quad \forall i \in \{1, \ldots, n\}. \tag{6}$$

For a given graph $\mathcal{G} \in \Gamma_n$ and a full rank diagonal matrix $\Upsilon \in \mathbb{R}^{n \times n}$, let us define the *generalized Laplacian flow* by

$$\dot{x} = -\mathcal{L}(\mathcal{G})\Upsilon x. \tag{7}$$

Lemma 1 (Generalized Laplacian Flow) *For the generalized Laplacian flow, the following statements hold*:

(1) *The equilibrium points are given by*

$$\mathcal{E} = \left\{\alpha \Upsilon^{-1} \mathbf{1}_n \mid \alpha \in \mathbb{R}\right\}.$$

(2) *The solutions converge to the set $\mathcal{E}$ if and only if $\Upsilon > 0$.*

Proof We start by establishing the first statement. The equilibrium points are given by

$$\Upsilon x \in \ker\left(\mathcal{L}(\mathcal{G})\right). \tag{8}$$

Since Υ is full rank, the set in (8) is equivalent to the set $\mathcal{E}$.

To prove the second statement, we start by establishing the sufficiency. We consider a Lyapunov function $V(x) = x^T \Upsilon \mathcal{L}(\mathcal{G}) \Upsilon x$. We note that $V(x) \geq 0$ and $V(z) = 0$ only if $z \in \mathcal{E}$. The Lie derivative of this Lyapunov function along the generalized Laplacian flow is given by

$$\dot{V} = -2x^T \Upsilon \mathcal{L}(\mathcal{G}) \Upsilon \mathcal{L}(\mathcal{G}) \Upsilon x = -2\left\| \Upsilon^{\frac{1}{2}} \mathcal{L}(\mathcal{G}) \Upsilon x \right\|^2 \leq 0.$$

Hence, the Lyapunov function is monotonically non-increasing along the generalized Laplacian flow. The proof for convergence to the set $\mathcal{E}$ is similar to Exercise 1.25 in Bullo et al. (2009).

To establish necessity, assume that some entry of Υ is negative. Without loss of generality we assume that the ith diagonal entry is $\upsilon_i < 0$. We observe that

$$e_i^T \mathcal{L}(\mathcal{G})\Upsilon e_i = \upsilon_i e_i^T \mathcal{L}(\mathcal{G}) e_i < 0,$$

where e_i is the ith element of the canonical basis of $\mathbb{R}^n$. Hence, the matrix $-\mathcal{L}(\mathcal{G})\Upsilon$ has at least one positive eigenvalue, which implies that the generalized Laplacian flow is unstable. We further observe that Υ cannot have a zero entry, since it is a full rank matrix, which concludes the proof. □

Before we analyze the absolute nonlinear flow with pitchfork nonlinearity, we introduce some useful notation. Given $\gamma \in \mathbb{R}_{>0}$, define $f_0, f_\pm : [-\sqrt{4\gamma/3}, \sqrt{4\gamma/3}] \to \mathbb{R}$ by

$$f_0(\beta) = \beta, \quad \text{and} \quad f_\pm(\beta) = -\frac{\beta}{2} \pm \sqrt{\gamma - \frac{3}{4}\beta^2}.$$

Theorem 1 (Absolute nonlinear flow with pitchfork nonlinearity) *For the absolute nonlinear flow with pitchfork nonlinearity, the following statements hold*:

(1) *Equilibrium points:*
For $\gamma \leq 0$, the set of equilibrium points is

$$\mathcal{E}_c = \operatorname{diag}\big(\mathbb{R}^n\big). \tag{9}$$

For $\gamma > 0$, the set of equilibrium points is

$$\mathcal{E}_b = \big\{ y \in \mathbb{R}^n \mid y_1, \ldots, y_n \in \big\{ f_-(\beta), f_0(\beta), f_+(\beta) \big\} \text{ and } \beta \in \big[-\sqrt{4\gamma/3}, \sqrt{4\gamma/3}\big] \big\}.$$

(2) *Consensus:*
For $\gamma \leq 0$, each trajectory converges to some point in the set $\mathcal{E}_c$.
(3) *Bifurcation:*
For $\gamma > 0$, each equilibrium point $x^* \in \mathcal{E}_b$ is locally stable if and only if $3x_i^{*2} > \gamma$ for each $i \in \{1, \ldots, n\}$.

Alternative Characterization of Equilibrium Points Let Ξ be the set of n-dimensional vectors with entries in $\{-, 0, +\}$, whose cardinality is 3^n. Therefore, $\xi \in \Xi$ is an n-dimensional multi-index with indices in alphabet $\{-, 0, +\}$. For any $\xi \in \Xi$, define $f_\xi : [-\sqrt{4\gamma/3}, \sqrt{4\gamma/3}] \to \mathbb{R}^n$ by

$$f_\xi(\beta) = \big(f_{\xi_1}(\beta), \ldots, f_{\xi_n}(\beta)\big) \in \mathbb{R}^n.$$

The set $\mathcal{E}_b$ can be interpreted as the union of three curves in the following way:

$$\mathcal{E}_b = \bigcup_{\xi \in \Xi} f_\xi\big([-\sqrt{4\gamma/3}, \sqrt{4\gamma/3}]\big).$$

(Here we let $g(A)$ denote the image of a function $g : A \to \mathbb{R}$.)

Proof We start by determining the equilibrium points for (5), which are given by

$$\begin{aligned} &\gamma x - \operatorname{diag}(x)^3 \mathbf{1}_n \in \ker\big(\mathcal{L}(\mathcal{G})\big), \\ &\quad \Longrightarrow \gamma x_i - x_i^3 = \alpha, \quad \forall i \in \{1, \dots, n\}, \quad \text{and } \alpha \in \mathbb{R}. \end{aligned} \tag{10}$$

We observe that (10) is a cubic equation and, hence, has at least one real root β (say). The other roots of (10) can be determined in terms of β, and they are given by

$$x_i = -\frac{\beta}{2} \pm \sqrt{\gamma - \frac{3}{4}\beta^2}, \quad \forall i \in \{1, \dots, n\}. \tag{11}$$

We observe that the roots given in (11) are complex if $\gamma \le 0$. Hence, for $\gamma \le 0$, the equilibrium points are given by the set $\mathcal{E}_c$. It follows from (11) that for $\gamma > 0$, $\mathcal{E}_b$ is the set of equilibrium points.

To establish the second statement, we consider a Lyapunov function $V(x) = x^T \mathcal{L}(\mathcal{G}) x$. We observe that, for $\gamma \le 0$, the Lie derivative of this Lyapunov function along the absolute nonlinear flow with pitchfork nonlinearity is given by

$$\dot{V}(x) = 2\gamma x^T \mathcal{L}(\mathcal{G}) x - 2x^T \mathcal{L}(\mathcal{G}) \operatorname{diag}(x)^3 \mathbf{1}_n \le 2\gamma x^T \mathcal{L}(\mathcal{G}) x \le 0,$$

which establishes the stability of each point in the set $\mathcal{E}_c$. The proof of convergence is similar to Exercise 1.25 in Bullo et al. (2009).

To establish the third statement, we linearize the absolute nonlinear flow with pitchfork nonlinearity about an equilibrium point x^* to get

$$\dot{x} = \mathcal{L}(\mathcal{G})\big(\gamma I - 3 \operatorname{diag}(x^*)^2\big) x =: \mathcal{L}(\mathcal{G}) \Upsilon x,$$

where Υ is a diagonal matrix. From Lemma 1, it follows that each equilibrium point $x^* \in \mathcal{E}_b$ is locally stable if and only if Υ is negative definite, which concludes the proof. □

Remark 1 The results in Theorem 1 hold for any directed graph with at least one globally reachable node.

Conjecture 1 (Completeness) *Given a $\gamma \in \mathbb{R}$, the union of the basins of attraction of all the stable equilibrium points of the absolute nonlinear flow with pitchfork nonlinearity is $\mathbb{R}^n \setminus \mathcal{Z}$, where $\mathcal{Z}$ is a measure zero set.*

Conjecture 2 (Switching topology) *The results in Theorem 1 hold for a network with switching topology $\mathcal{G}_k \in \Gamma_n$, $k \in \mathbb{N}$.*

Discussion (Absolute nonlinear system with pitchfork nonlinearity) We determined the equilibrium points of the absolute nonlinear flow with pitchfork nonlinearity and established their stability in Theorem 1. Now we study this system on some low

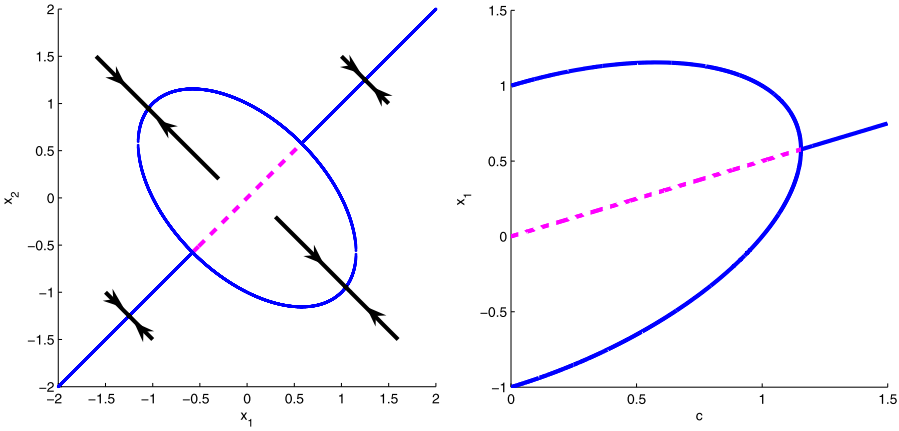

(a) Equilibrium points (b) Bifurcation diagram

Fig. 1 (Color online) Absolute nonlinear flow with pitchfork nonlinearity on a graph with two nodes and $\gamma = 1$. (**a**) The unstable equilibrium points are shown as a *magenta colored dashed line*, while the stable ones are shown in *blue colored solid lines*. (**b**) The bifurcation diagram for the reduced system. Notice the pitchfork bifurcation at $c = 2/\sqrt{3}$

order graphs to better understand the underlying dynamics. We start with a graph with two nodes. For $\gamma \leq 0$, the set of equilibrium points of this system is the set $\mathcal{C}_2 = \{(x_1, x_2) \in \mathbb{R}^2 \mid x_1 = x_2\}$, which are all stable, while for $\gamma > 0$, the set of equilibrium points is $\mathcal{C}_2 \cup \mathcal{E}_2$, where $\mathcal{E}_2 = \{(x_1, x_2) \in \mathbb{R}^2 \mid x_1^2 + x_2^2 + x_1 x_2 = \gamma\}$. The set of equilibrium points for $\gamma = 1$ is shown in Fig. 1(a). The subset of the consensus set $\mathcal{C}_2$ belonging to the convex hull of the set $\mathcal{E}_2$ is unstable. As γ is decreased, the ellipse of equilibrium points shrinks in size, disappearing at $\gamma = 0$.

Observe that $x_1 + x_2$ is an invariant along any trajectory of the system, and it can be utilized to reduce the dimension of the system. For the reduced system $x_1 + x_2 \equiv c$ is a parameter, and it turns out that a pitchfork bifurcation is observed at $c = \sqrt{4\gamma/3}$. The corresponding bifurcation diagram for $\gamma = 1$ is shown in Fig. 1(b). For $c \geq \sqrt{4\gamma/3}$, the only equilibrium point of the system is at $x = c/2$. For $c < \sqrt{4\gamma/3}$, this equilibrium point loses its stability and two new stable equilibrium points appear in the system. This is a pitchfork bifurcation.

We now consider a line graph with three nodes. For $\gamma \leq 0$, the set of equilibrium points is $\mathcal{C}_3 = \{(x_1, x_2, x_3) \in \mathbb{R}^3 \mid x_1 = x_2 = x_3\}$, which are all stable for $\gamma < 0$. For $\gamma > 0$, the set of equilibrium points is $\mathcal{C}_3 \cup \mathcal{E}_3$, where $\mathcal{E}_3 = \{(x_1, x_2, x_3) \in \mathbb{R}^3 \mid x_1^2 + x_2^2 + x_1 x_2 = \gamma,\ \text{or}\ x_1^2 + x_3^2 + x_1 x_3 = \gamma,\ \text{or}\ x_2^2 + x_3^2 + x_3 x_3 = \gamma\}$; the points $(x, x, x) \in \mathcal{E}_3$ are unstable for $|x| < \sqrt{\gamma/3}$ and stable for $|x| > \sqrt{\gamma/3}$. The set of equilibrium points for $\gamma = 1$ is shown in Fig. 2(a). Similar to the two node case, $x_1 + x_2 + x_3$ is an invariant along any trajectory of the system, and this can be utilized to reduce the dimension of the system. For the reduced system $x_1 + x_2 + x_3 \equiv c$ is a parameter, and very interesting behaviors are observed as this parameter is varied. We note that the equilibrium at $(c/3, c/3)$ corresponds to the consensus state. For $c = 0$ the set of equilibrium points is $(0, 0) \cup \mathcal{E}_2$, where $\mathcal{E}_2 = \{(x_1, x_2) \in \mathbb{R}^2 \mid x_1^2 + x_2^2 + x_1 x_2 = \gamma\}$. Furthermore, each point in the set $\mathcal{E}_2$ is stable, while the equilibrium point $(0, 0)$ is a

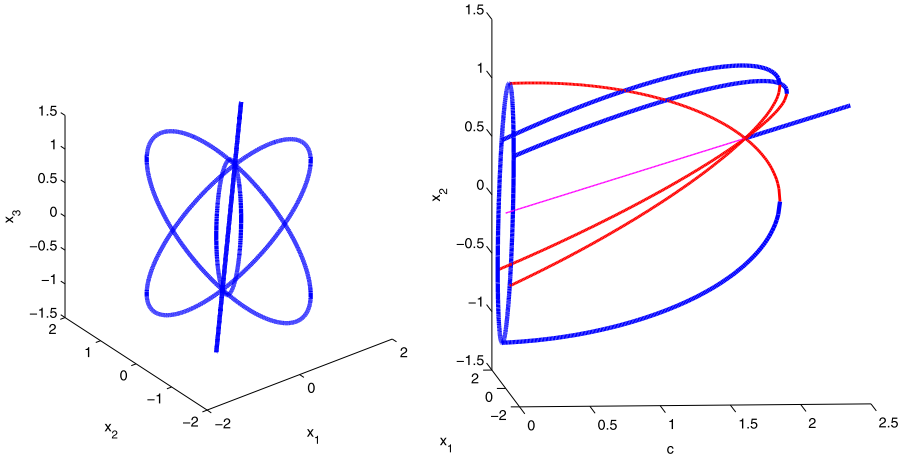

(a) Equilibrium points (b) Bifurcation diagram

Fig. 2 Absolute nonlinear flow with pitchfork nonlinearity on a line graph with three nodes and $\gamma = 1$. (**a**) The equilibrium points are comprised of three ellipses and a line. (**b**) The bifurcation diagram for the reduced system. Notice the S_3-symmetric transcritical bifurcation at $c = \sqrt{3}$, and the saddle-node bifurcations at $c = 2$

source (see Fig. 3(a)). As the value of c is increased from zero, the reduced system has seven equilibrium points, three of which are sinks, three are saddle points, and one is a source (see Fig. 3(b)). As the value of c is further increased, the three saddle points move toward the source, reaching it at $c = \sqrt{3\gamma}$ at an S_3-symmetric transcritical bifurcation (Ashwin et al. 2008; Kimura and Moehlis 2008). As the saddle points cross the source, i.e., for $c > \sqrt{3\gamma}$, the source becomes a sink (see Fig. 3(c)), and the three saddle points move toward the other three sinks. At $c = 2\sqrt{\gamma}$, the three saddles meet the three sinks and annihilate each other in saddle-node bifurcations. For $c > 2$, there is only one equilibrium point in the system, which is a sink (see Fig. 3(d)). A bifurcation diagram for $\gamma = 1$ is shown in Fig. 2(b). It can be seen that at $c = \sqrt{3}$, the three saddle points (shown as red color lines with medium thickness) reach the source (shown as magenta color thin line), and thus convert it into a sink (shown as blue color thick lines). The annihilation of the saddle points and sinks through saddle-node bifurcations can also be seen at $c = 2$.

Finally, we consider a ring graph with three nodes. We proved in Theorem 1 that the set of equilibrium points and their stability properties are invariant over the set Γ_n, but the trajectories and the basins of attraction of these equilibrium points do change with the graph topology. In Fig. 4, we show the phase plot for the reduced absolute nonlinear flow with pitchfork nonlinearity on a ring graph with three nodes reduced on the hyperplane $x_1 + x_2 + x_3 = 0.5$. Observe that the trajectories and the basins of attraction of the equilibrium points are different from those for the line graph in Fig. 3(b).

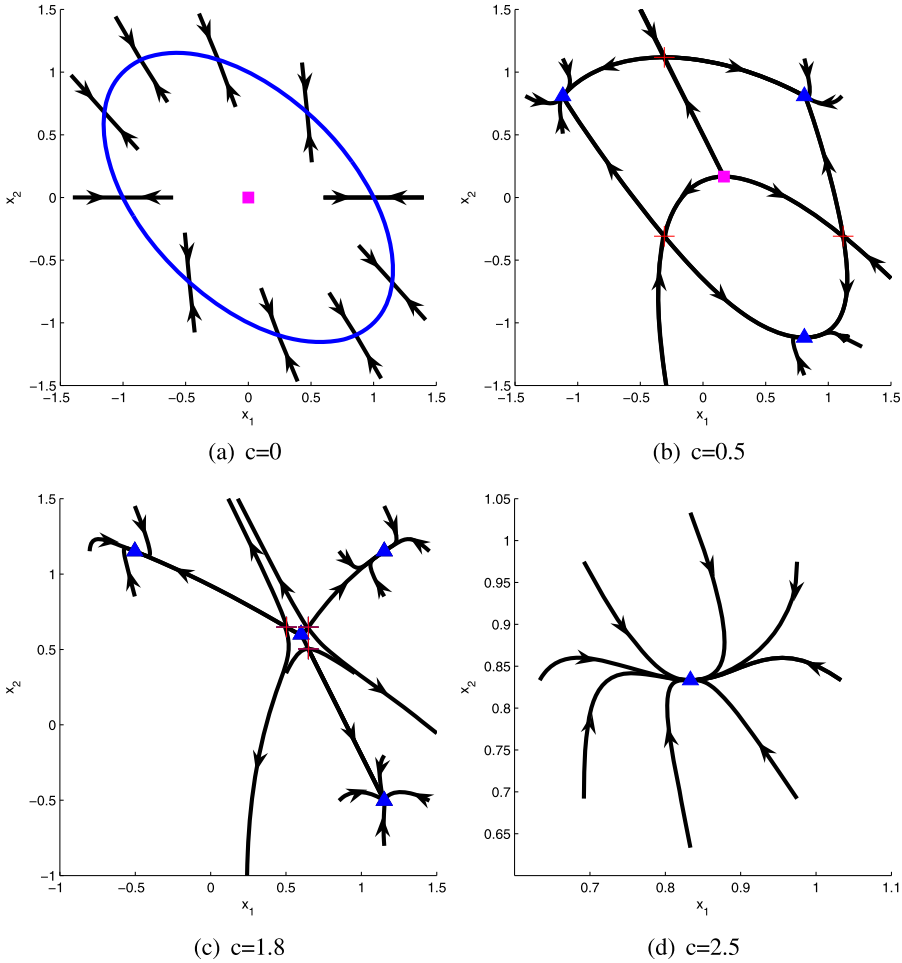

(a) c=0 (b) c=0.5

(c) c=1.8 (d) c=2.5

Fig. 3 (Color online) Phase plots for the reduced absolute nonlinear flow on a line graph with three nodes and $\gamma = 1$. The stable equilibrium points are shown in *blue*. The isolated sinks are shown as *blue triangles*, the sources are shown as *magenta squares*, and the saddles are shown as *red plus signs*. (**a**) An ellipse is the set of the stable equilibrium points, and the consensus point is the source. (**b**) Three sinks and three saddles are present. The consensus point remains a source. (**c**) The saddles have crossed the consensus point and turned it into a sink, and have moved further toward the other three sinks. (**d**) The three saddles have annihilated the three sinks, and the consensus point is a global sink

4.2 Relative Nonlinear Flow with Pitchfork Nonlinearity

Given a connected undirected graph $\mathcal{G} \in \Gamma_n$, and $\gamma \in \mathbb{R}$, the relative nonlinear flow with pitchfork nonlinearity, $\forall i \in \{1, \ldots, n\}$, is

$$\dot{x}_i = \gamma \sum_{j \in \mathrm{adj}(i)} (x_i - x_j) - \sum_{j \in \mathrm{adj}(i)} (x_i - x_j)^3. \tag{12}$$

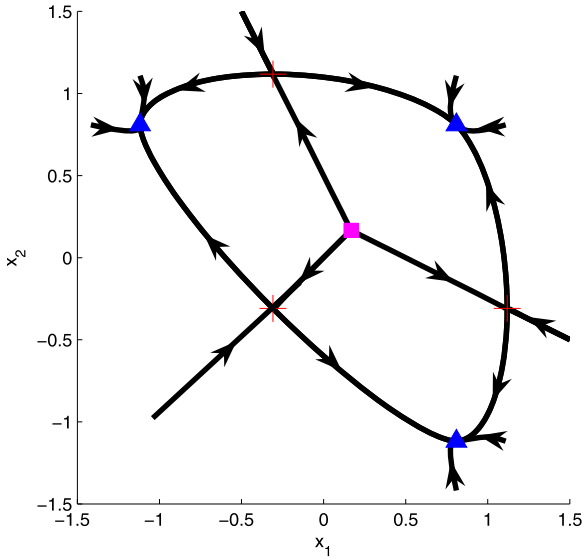

Fig. 4 (Color online) The reduced absolute nonlinear flow with pitchfork nonlinearity on a ring graph with three nodes, $\gamma = 1$, and $x_1 + x_2 + x_3 = 0.5$. The sinks are shown as *blue triangles*, the saddles are shown as *red plus signs*, and the source is shown as a *magenta square*

Note that for the relative nonlinear flow with pitchfork nonlinearity, $\sum_{i=1}^{n} \dot{x}_i = 0$, which implies that $\sum_{i=1}^{n} x_i$ is invariant along any trajectory of the system. This system is, in general, hard to characterize. In the following discussion we present this class of dynamics on some low order graphs.

Discussion (Relative nonlinear flow with pitchfork nonlinearity) We first study the relative nonlinear flow with pitchfork nonlinearity on a line graph with two nodes. For $\gamma \leq 0$, the set of equilibrium points for this system is the consensus set, i.e., $\mathcal{C}_2 = \{(x_1, x_2) \in \mathbb{R}^2 \mid x_1 = x_2\}$ and each equilibrium point is stable. For $\gamma > 0$, the set of equilibrium points is $\mathcal{C}_2 \cup \mathcal{A}_2$, where $\mathcal{A}_2 = \{(x_1, x_2) \mid x_1 - x_2 = \pm\sqrt{\gamma}\}$. Moreover, for $\gamma > 0$ each point in $\mathcal{A}_2$ is stable, while each point in $\mathcal{C}_2$ is unstable. A phase plot of this system is shown in Fig. 5.

We now study this system on a line graph with three nodes. For $\gamma \leq 0$, the set of equilibrium points of this system is the consensus set, i.e., $\mathcal{C}_3 = \{(x_1, x_2, x_3) \in \mathbb{R}^3 \mid x_1 = x_2 = x_3\}$, which is stable. For $\gamma > 0$, the set of equilibrium points is $\mathcal{C}_3 \cup \mathcal{A}_3$, where

$$\begin{aligned}\mathcal{A}_3 = \Bigg\{ &\left(\frac{c+3\sqrt{\gamma}}{3}, \frac{c}{3}, \frac{c-3\sqrt{\gamma}}{3}\right), \left(\frac{c+\sqrt{\gamma}}{3}, \frac{c-2\sqrt{\gamma}}{3}, \frac{c+\sqrt{\gamma}}{3}\right), \\ &\left(\frac{c-3\sqrt{\gamma}}{3}, \frac{c}{3}, \frac{c+3\sqrt{\gamma}}{3}\right), \left(\frac{c-\sqrt{\gamma}}{3}, \frac{c+2\sqrt{\gamma}}{3}, \frac{c-\sqrt{\gamma}}{3}\right), \\ &\left(\frac{c+2\sqrt{\gamma}}{3}, \frac{c-\sqrt{\gamma}}{3}, \frac{c-\sqrt{\gamma}}{3}\right), \left(\frac{c-2\sqrt{\gamma}}{3}, \frac{c+\sqrt{\gamma}}{3}, \frac{c+\sqrt{\gamma}}{3}\right), \\ &\left(\frac{c+\sqrt{\gamma}}{3}, \frac{c+\sqrt{\gamma}}{3}, \frac{c-2\sqrt{\gamma}}{3}\right), \left(\frac{c-\sqrt{\gamma}}{3}, \frac{c-\sqrt{\gamma}}{3}, \frac{c+2\sqrt{\gamma}}{3}\right), \ c \in \mathbb{R} \Bigg\}.\end{aligned}$$

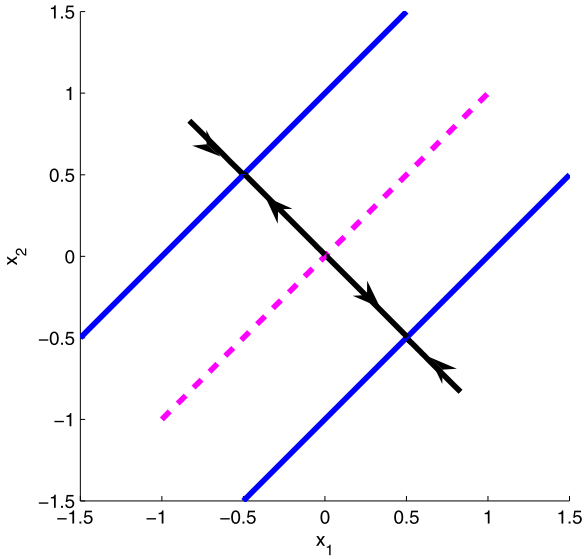

Fig. 5 (Color online) Phase plot for relative nonlinear flow with pitchfork nonlinearity on a graph with two nodes and $\gamma = 1$. The consensus set (shown as *magenta colored dashed line*) is unstable, while two sets (shown as *blue colored solid line*) are stable

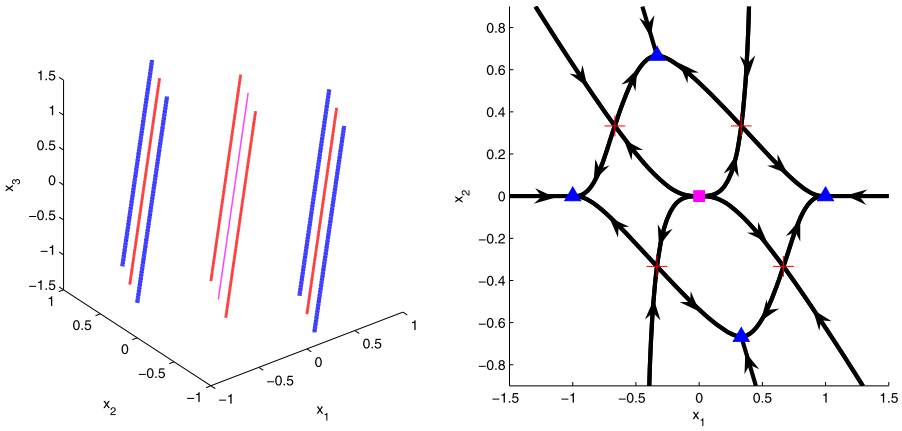

(a) Equilibrium points (b) Phase plot

Fig. 6 (Color online) The relative nonlinear flow with pitchfork nonlinearity on a line graph with three nodes and $\gamma = 1$. (**a**) The set of equilibrium points consists of nine lines. (**b**) The phase plot of the reduced system for $c = 0$. The system is comprised of nine equilibrium points. The consensus point (shown as magenta square) is a source, four equilibrium points are sinks (shown as *blue triangles*), and four equilibrium points are saddle points (shown as *red plus signs*)

These equilibrium points are shown in Fig. 6(a). We now exploit the fact that the sum of the states is invariant over a trajectory to reduce the dimension of the system. The phase plot of the reduced system is shown in Fig. 6(b). Notice that the reduced system is comprised of four sinks, four saddle points, and a source (consensus point).

Finally, we study this system on a ring graph with three nodes. For $\gamma \leq 0$, the set of equilibrium points of this system is the consensus set, i.e., $\mathcal{C}_3 = \{(x_1, x_2, x_3) \in \mathbb{R}^3 \mid x_1 = x_2 = x_3\}$, which are stable for $\gamma < 0$. For $\gamma > 0$, the set of equilibrium

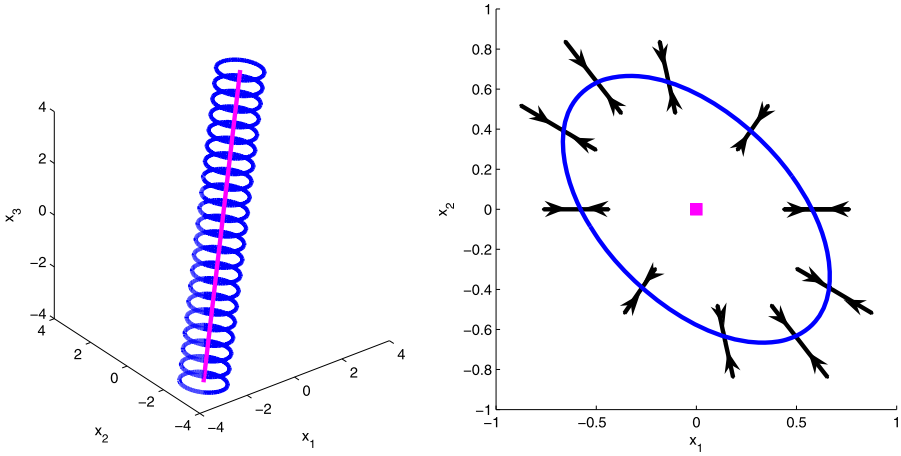

(a) Equilibrium points (b) Phase plot

Fig. 7 (Color online) The relative nonlinear flow with pitchfork nonlinearity on a ring graph with three nodes and $\gamma = 1$. (**a**) The set of equilibrium points is an elliptic cylinder (represented in the figure by *rings*) and a line. (**b**) The phase plot of the reduced system for $c = 0$. Each point of the ellipse is stable, while the consensus point (shown as a *magenta square*) is a source

points is $\mathcal{C}_3 \cup \mathcal{E}_{\text{cyl}}$, where

$$\mathcal{E}_{\text{cyl}} = \left\{ x_1, x_2, x_3 \mid x_1^2 + x_2^2 + x_1 x_2 - c x_1 - c x_2 + \frac{c^2 - \gamma}{3} = 0, \text{ and } x_1 + x_2 + x_3 = c,\ c \in \mathbb{R} \right\}.$$

These equilibrium points are shown in Fig. 7(a). Again, the invariance of the sum of the states along a trajectory is exploited to reduce the dimension of the system. The phase plot of the reduced system is shown in Fig. 7(b). Note that each point of $\mathcal{E}_{\text{cyl}}$ projected on the reduced space is stable, while the consensus point is a source.

4.3 Disagreement Nonlinear Flow with Pitchfork Nonlinearity

Given a connected undirected graph $\mathcal{G} \in \Gamma_n$, and $\gamma \in \mathbb{R}$, the disagreement nonlinear flow with pitchfork nonlinearity is

$$\dot{x} = \gamma \mathcal{L}(\mathcal{G}) x - \big(\operatorname{diag}\big(\mathcal{L}(\mathcal{G}) x\big)\big)^3 \mathbf{1}_n. \tag{13}$$

In components, the above dynamics, $\forall i \in \{1, \ldots, n\}$, are given by

$$\dot{x_i} = \gamma \sum_{j \in \operatorname{adj}(i)} (x_i - x_j) - \left(\sum_{j \in \operatorname{adj}(i)} (x_i - x_j) \right)^3. \tag{14}$$

Before we analyze the disagreement nonlinear flow with pitchfork nonlinearity, we introduce the following notation. We partition the Laplacian matrix in the following

way:

$$\mathcal{L}(\mathcal{G}) = \begin{bmatrix} L_{n-1} & L_{*,n} \\ L_{n,*} & L_{n,n} \end{bmatrix}, \tag{15}$$

where $L_{n-1} \in \mathbb{R}^{(n-1)\times(n-1)}$.

We also construct a transformation matrix $P \in \mathbb{R}^{n\times n}$ in the following way:

$$P = \begin{bmatrix} L_{n-1} & L_{*,n} \\ \mathbf{1}_{n-1}^T & 1 \end{bmatrix}. \tag{16}$$

The last row of the transformation matrix P is chosen to be the basis of the kernel of the Laplacian matrix $\mathcal{L}(\mathcal{G})$, for $\mathcal{G} \in \Gamma_n$. Hence, a coordinate transform through matrix P separates the center manifold and the stable/unstable manifold. Now, we state some properties of the transformation matrix P.

Lemma 2 (Properties of the transformation matrix) *Given a graph $\mathcal{G} \in \Gamma_n$, then for the transformation matrix P defined in* (16), *the following statements hold*:

(1) *The submatrix L_{n-1} is symmetric positive definite.*
(2) *The transformation matrix P is full rank.*
(3) *The inverse of the transformation matrix satisfies*

$$\mathbf{1}_n^T P^{-1} = e_n^T, \quad \textit{and} \quad P^{-1} e_n = \frac{1}{n}\mathbf{1}_n,$$

where $e_n = [0 \ \dots \ 0 \ 1]^T$.

Proof We start by establishing the first statement. We define a matrix T by

$$T = \begin{bmatrix} I_{n-1} & 0 \\ \mathbf{1}_{n-1}^T & 1 \end{bmatrix},$$

and note that

$$T\mathcal{L}(\mathcal{G}) = \begin{bmatrix} L_{n-1} & L_{*,n} \\ 0 & 0 \end{bmatrix}.$$

The matrix T is full rank, hence $\ker(T\mathcal{L}(\mathcal{G})) = \ker(\mathcal{L}(\mathcal{G}))$. Moreover, from Theorem 1.37 in Bullo et al. (2009), we know that for a connected undirected graph, rank $(\mathcal{L}(\mathcal{G})) = n-1$. Therefore, rank $(T\mathcal{L}(\mathcal{G})) = n-1$. We also note that $L_{n-1}\mathbf{1}_{n-1} = -L_{*,n}$. Hence, L_{n-1} must have full rank. Furthermore, L_{n-1} is a principal minor of the positive semidefinite matrix $\mathcal{L}(\mathcal{G})$. Hence, L_{n-1} is positive definite.

To establish the second statement, we construct a matrix $\Gamma = [\mathcal{L}(\mathcal{G}) \ \mathbf{1}_n]^T$. Since $\mathbf{1}_n \in \ker(\mathcal{L}(\mathcal{G}))$, Γ has full row rank. We also construct a matrix $\tilde{T}$ as

$$\tilde{T} = \begin{bmatrix} I_{n-1} & 0 & 0 \\ \mathbf{1}_{n-1}^T & 1 & 0 \\ 0 & 0 & 1 \end{bmatrix},$$

and note that

$$\tilde{T}\Gamma = \begin{bmatrix} L_{n-1} & L_{*,n} \\ 0 & 0 \\ \mathbf{1}_{n-1}^T & 1 \end{bmatrix}.$$

An argument similar to the one in the proof of the previous statement establishes the second statement.

To prove the third statement, we note that the inverse of transformation matrix P is given by

$$P^{-1} = \begin{bmatrix} (L_{n-1} - L_{*,n}\mathbf{1}_{n-1}^T)^{-1} & \frac{1}{n}\mathbf{1}_{n-1} \\ -\mathbf{1}_{n-1}^T(L_{n-1} - L_{*,n}\mathbf{1}_{n-1}^T)^{-1} & \frac{1}{n} \end{bmatrix}. \tag{17}$$

It follows immediately from (17) that $\mathbf{1}_n^T P^{-1} = e_n$ and $P^{-1}e_n = \frac{1}{n}\mathbf{1}_n$. This concludes the proof of the third and the last statement. □

Theorem 2 (Disagreement nonlinear flow with pitchfork nonlinearity) *For the disagreement nonlinear flow with pitchfork nonlinearity, the following statements hold*:

Equilibrium points:

(1) *For $\gamma \le 0$, the set of equilibrium points is*

$$\mathcal{F}_c = \operatorname{diag}(\mathbb{R}^n).$$

(2) *For $\gamma > 0$, the set of equilibrium points is*

$$\mathcal{F}_b = \left\{ P^{-1}y \;\middle|\; y \in \mathbb{R}^n,\, y_1, \ldots, y_{n-1} \in \{0, -\sqrt{\gamma}, \sqrt{\gamma}\},\, y_n \text{ is arbitrary and } \sum_{i=1}^{n-1} y_i \in \{0, -\sqrt{\gamma}, \sqrt{\gamma}\} \right\}.$$

Consensus:

For $\gamma \le 0$, each trajectory converges to some point in the set $\mathcal{F}_c$.

Bifurcation:

(1) *For $\gamma > 0$, and n even, the set of locally stable equilibrium points is*

$$\bar{\mathcal{F}}_b = \left\{ P^{-1}y \;\middle|\; y \in \mathbb{R}^n,\, y_1, \ldots, y_{n-1} \in \{-\sqrt{\gamma}, \sqrt{\gamma}\},\, y_n \text{ is arbitrary, and } \sum_{i=1}^{n-1} y_i \in \{-\sqrt{\gamma}, \sqrt{\gamma}\} \right\}.$$

Moreover, each equilibrium point $x^* \in \mathcal{F}_b \setminus \bar{\mathcal{F}}_b$ is unstable.

(2) *For $\gamma > 0$, and odd $n > 1$, each equilibrium point $x^* \in \mathcal{F}_b$ is unstable.*

Proof We transform the coordinates to $y = Px$ and observe that in the new coordinates equation (13) transforms to

$$P^{-1}\dot{y} = \begin{bmatrix} \gamma y_1 - y_1^3 \\ \vdots \\ \gamma y_{n-1} - y_{n-1}^3 \\ -\gamma \sum_{i=1}^{n-1} y_i + (\sum_{i=1}^{n-1} y_i)^3 \end{bmatrix}. \tag{18}$$

We construct a matrix Q by

$$Q = \begin{bmatrix} I_{n-1} & 0 \\ \mathbf{1}_{n-1}^T & 1 \end{bmatrix},$$

and invoke Lemma 2 to observe that

$$QP^{-1} = \begin{bmatrix} (L_{n-1} - L_{*,n}\mathbf{1}_{n-1}^T)^{-1} & \frac{1}{n}\mathbf{1}_{n-1} \\ 0 & 1 \end{bmatrix}.$$

We multiply each side of (18) with Q to get

$$\left(L_{n-1} - L_{*,n}\mathbf{1}_{n-1}^T\right)^{-1} \begin{bmatrix} \dot{y}_1 \\ \vdots \\ \dot{y}_{n-1} \end{bmatrix} = \begin{bmatrix} \gamma y_1 - y_1^3 \\ \vdots \\ \gamma y_{n-1} - y_{n-1}^3 \end{bmatrix} - \frac{1}{n}\mathbf{1}_{n-1}\dot{y}_n,$$

$$\dot{y}_n = -\sum_{i=1}^{n-1} y_i^3 + \left(\sum_{i=1}^{n-1} y_i\right)^3.$$

The above set of equations is equivalent to

$$\begin{bmatrix} \dot{y}_1 \\ \vdots \\ \dot{y}_{n-1} \end{bmatrix} = \left(L_{n-1} - L_{*,n}\mathbf{1}_{n-1}^T\right) \begin{bmatrix} \gamma y_1 - y_1^3 \\ \vdots \\ \gamma y_{n-1} - y_{n-1}^3 \end{bmatrix} + L_{*,n}\dot{y}_n, \tag{19}$$

$$\dot{y}_n = -\sum_{i=1}^{n-1} y_i^3 + \left(\sum_{i=1}^{n-1} y_i\right)^3. \tag{20}$$

The equilibrium point of the system in (19), for each $i \in \{1, \ldots, n-1\}$, is given by

$$y_i^* \in \begin{cases} \{0\}, & \text{if } \gamma \le 0, \\ \{0, \pm\sqrt{\gamma}\} & \text{if } \gamma > 0. \end{cases}$$

The equilibrium points thus obtained should be consistent with the equilibrium condition of (20). Substitution of these equilibrium points into (20) yields

$$\sum_{i=1}^{n-1} y_i \in \{0, \pm\sqrt{\gamma}\}.$$

The equilibrium value of y_n is a free parameter and can take any value $\beta \in \mathbb{R}$.

The proof of the stability of the set $\mathcal{F}_c$ is similar to the Lyapunov function-based proof in Theorem 1. To prove the local stability of each equilibrium point $x^* \in \bar{\mathcal{F}}_b$, for n even, we shift the origin of (19) and (20), defining new coordinates as

$$(\zeta_1, \zeta_2)^T = (\zeta_{11}, \ldots, \zeta_{1n-1}, \zeta_2)^T = y - y^*,$$

where $P^{-1}y^* \in \bar{\mathcal{F}}_b$. In these new coordinates, (19) and (20) become

$$\begin{bmatrix} \dot{\zeta}_1 \\ \dot{\zeta}_2 \end{bmatrix} = \begin{bmatrix} -2\gamma L_{n-1}(I + \mathbf{1}_{n-1}\mathbf{1}_{n-1}^T) & 0 \\ 0 & 0 \end{bmatrix} \begin{bmatrix} \zeta_1 \\ \zeta_2 \end{bmatrix} + \begin{bmatrix} \bar{g}_1(\zeta_1) \\ \bar{g}_2(\zeta_2) \end{bmatrix}, \tag{21}$$

where $\bar{g}_1 : \mathbb{R}^{n-1} \to \mathbb{R}^{n-1}$ and $\bar{g}_2 : \mathbb{R}^{n-1} \to \mathbb{R}$ satisfy equation (3).

The dynamics of (21) are similar to the dynamics of (2), and $\zeta_1 = h(\zeta_2) = 0$ is the center manifold. The ζ_2 dynamics on this manifold are neutrally stable. Hence, each equilibrium point $x^* \in \bar{\mathcal{F}}_b$ is locally stable.

Similarly, for n odd, expressing (19) and (20) in the new coordinates gives

$$\begin{bmatrix} \dot{\zeta}_1 \\ \dot{\zeta}_2 \end{bmatrix} = \begin{bmatrix} \gamma L_{n-1}(-2I + \mathbf{1}_{n-1}\mathbf{1}_{n-1}^T) & 0 \\ -3\gamma \mathbf{1}_{n-1}^T & 0 \end{bmatrix} \begin{bmatrix} \zeta_1 \\ \zeta_2 \end{bmatrix} + \begin{bmatrix} g_1(\zeta_1) \\ g_2(\zeta_2) \end{bmatrix}, \tag{22}$$

where $g_1 : \mathbb{R}^{n-1} \to \mathbb{R}^{n-1}$ and $g_2 : \mathbb{R}^{n-1} \to \mathbb{R}$ satisfy the conditions in equation (3). Since the matrix $-2I + \mathbf{1}_{n-1}\mathbf{1}_{n-1}^T$ has an eigenvalue at $n-3$, the equilibria are unstable for $n \geq 3$.

The instability of the set $\mathcal{F}_b \setminus \bar{\mathcal{F}}_b$ follows similarly. □

Remark 2 The absolute, relative and disagreement nonlinear flows can be studied with other normal forms for the bifurcations in scalar systems. For example, one may consider the transcritical nonlinearity $f_i : \mathbb{R} \to \mathbb{R}$ defined by $f_i(x) = \gamma x - x^2$, for all $i \in \{1, \ldots, n\}$, and some $\gamma \in \mathbb{R}$. It can be shown that, for $\gamma > 0$, the absolute nonlinear flow with transcritical nonlinearity converges to consensus under very restrictive conditions; otherwise, it is unstable. The disagreement nonlinear flow with transcritical nonlinearity is unstable for $\gamma > 0$.

5 Conclusions

In this paper, we considered three frameworks which define distributed nonlinear dynamics in multi-agent networks. We determined the set of equilibria that could be achieved through these dynamics, and examined their stability. We also described the

bifurcation behavior in multi-agent networks using these frameworks, and demonstrated a variety of interesting behaviors that can be achieved. These models could be used for the development of distributed protocols to achieve a certain configuration in a robotic network. Moreover, several physical and ecological systems lie in the category of relative nonlinear flow, e.g., power network models, and models for collective animal behavior; the analysis presented in this paper could be helpful for understanding these systems. Furthermore, the models presented in this paper could be used to design distributed systems with desired properties, e.g., one could design an artificial biological network to achieve a certain performance.

A number of extensions to the work presented here are possible. For example, the networks considered here are static. There is a high possibility that the described dynamics persist for networks with switching topology as well. Furthermore, the class of functions which yield stable equilibria is not well understood yet. It remains an open problem to characterize this. The passivity-based approach of Arcak (2007) could be helpful in ascertaining the stability for a general class of nonlinearities. Another future direction of research is to explore the dynamic behavior on graphs with special structures, e.g., graphs with symmetry.

Acknowledgements This work was supported in part by AFOSR MURI grant FA9550-07-1-0528.

References

Arcak, M.: Passivity as a design tool for group coordination. IEEE Trans. Autom. Control **52**(8), 1380–1390 (2007)

Ashwin, P., Burylko, O., Maistrenko, Y.: Bifurcation to heteroclinic cycles and sensitivity in three and four coupled phase oscillators. Physica D **237**(4), 454–466 (2008)

Bogacz, R., Brown, E., Moehlis, J., Holmes, P., Cohen, J.D.: The physics of optimal decision making: A formal analysis of performance in two-alternative forced choice tasks. Psychol. Rev. **113**(4), 700–765 (2006)

Bullo, F., Cortés, J., Martínez, S.: Distributed Control of Robotic Networks. Applied Mathematics Series. Princeton University Press, Princeton (2009). Available at http://www.coordinationbook.info

Couzin, I.D., Krause, J., Franks, N.R., Levin, S.A.: Effective leadership and decision-making in animal groups on the move. Nature **433**(7025), 513–516 (2005)

Dionne, B., Golubitsky, M., Stewart, I.: Coupled cells with internal symmetry. Nonlinearity **9**, 559–599 (1996)

Dörfler, F., Francis, B.: Geometric analysis of the formation problem for autonomous robots. IEEE Trans. Automat. Contol **55**(10), 2379–2384 (2010)

Fax, J.A., Murray, R.M.: Information flow and cooperative control of vehicle formations. IEEE Trans. Autom. Control **49**(9), 1465–1476 (2004)

Jadbabaie, A., Lin, J., Morse, A.S.: Coordination of groups of mobile autonomous agents using nearest neighbor rules. IEEE Trans. Autom. Control **48**(6), 988–1001 (2003)

Khalil, H.K.: Nonlinear Systems, 3rd edn. Prentice Hall, New York (2002)

Kimura, M., Moehlis, J.: Novel vehicular trajectories for collective motion from coupled oscillator steering control. SIAM J. Appl. Dyn. Syst. **7**(4), 1191–1212 (2008)

Kwatny, H., Pasrija, A., Bahar, L.: Static bifurcations in electric power networks: Loss of steady-state stability and voltage collapse. IEEE Trans. Circuits Syst. **33**(10), 981–991 (1986)

Lin, J., Morse, A.S., Anderson, B.D.O.: The multi-agent rendezvous problem. Part 1: The synchronous case. SIAM J. Control Optim. **46**(6), 2096–2119 (2007)

Lorenz, J.: Continuous opinion dynamics under bounded confidence: A survey. Int. J. Mod. Phys. C **18**(12), 1819–1838 (2007)

Nabet, B., Leonard, N.E., Couzin, I.D., Levin, S.A.: Dynamics of decision making in animal group motion. J. Nonlinear Sci. **19**(4), 399–435 (2009)

Olfati-Saber, R., Fax, J.A., Murray, R.M.: Consensus and cooperation in networked multi-agent systems. Proc. IEEE **95**(1), 215–233 (2007)

Olfati-Saber, R., Murray, R.M.: Consensus problems in networks of agents with switching topology and time-delays. IEEE Trans. Autom. Control **49**(9), 1520–1533 (2004)

Olien, L., Bélair, J.: Bifurcations, stability, and monotonicity properties of a delayed neural network model. Physica D **102**(3-4), 349–363 (1997)

Papachristodoulou, A., Jadbabaie, A.: Synchronization in oscillator networks with heterogeneous delays, switching topologies and nonlinear dynamics. In: IEEE Conf. on Decision and Control, San Diego, CA, December 2006, pp. 4307–4312 (2006)

Poulakakis, I., Scardovi, L., Leonard, N.E.: Coupled stochastic differential equations and collective decision making in the Two-Alternative Forced-Choice task. In: American Control Conference, pp. 69–74 (2010)

Roxin, A., Ledberg, A.: Neurobiological models of two-choice decision making can be reduced to a one-dimensional nonlinear diffusion equation. PLoS Comput. Biol. **4**(3), e1000046 (2008)

Spanos, D.P., Olfati-Saber, R., Murray, R.M.: Approximate distributed Kalman filtering in sensor networks with quantifiable performance. In: Symposium on Information Processing of Sensor Networks, Los Angeles, CA, April 2005, pp. 133–139 (2005)

Srivastava, V., Moehlis, J., Bullo, F.: On bifurcations in nonlinear consensus networks. In: American Control Conference, Baltimore, MD, June 2010, pp. 1647–1652 (2010)

Strogatz, S.H.: Nonlinear Dynamics and Chaos: With Applications to Physics, Biology, Chemistry, and Engineering. Perseus Books Group, New York City (2000)

Tanner, H.G., Jadbabaie, A., Pappas, G.J.: Flocking in fixed and switching networks. IEEE Trans. Autom. Control **52**(5), 863–868 (2007)

Wei, J., Ruan, S.: Stability and bifurcation in a neural network model with two delays. Physica D **130**(3-4), 255–272 (1999)

Zou, F., Nossek, J.A.: Bifurcation and chaos in cellular neural networks. IEEE Trans. Circuits Syst. I, Fundam. Theory Appl. **40**(3), 166–173 (1993)